Optics & Laser Technology 142 (2021) 107230

Contents lists available at ScienceDirect

Optics and Laser Technology

journal homepage: www.elsevier.com/locate/optlastec

Full length article

Execution of all-optical Boolean OR logic using carrier reservoir semiconductor optical amplifier-assisted delayed interferometer

Amer Kotb [a,b,*], Kyriakos E. Zoiros [c], Wei Li [a,*]

[a] GPL, State Key Laboratory of Applied Optics, Changchun Institute of Optics, Fine Mechanics, and Physics, Chinese Academy of Sciences, Changchun 130033, China
[b] Department of Physics, Faculty of Science, University of Fayoum, Fayoum 63514, Egypt
[c] Lightwave Communications Research Group, Department of Electrical and Computer Engineering, School of Engineering, Democritus University of Thrace, Xanthi 67100, Greece

ARTICLE INFO

Keywords:
All-optical logic OR gate
Carrier reservoir semiconductor optical amplifier
Delayed interferometer

ABSTRACT

It is known that the conventional bulk semiconductor optical amplifier (SOA) faces the problem of the slow gain recovery time, which limits its application as a nonlinear element at higher data rates. Therefore, our goal is to find an alternative that works at higher rates with acceptable performance. In this paper, we employ, for the first time to our knowledge, a carrier reservoir SOA (CR-SOA) followed by a delayed interferometer (DI) to execute all-optically the Boolean OR operation at a data rate of 100 Gb/s. A performance comparison between the CR-SOA- and the conventional bulk SOA-based DI is made by studying the variation of the quality factor (Q-factor) against various key operating parameters, which include the transition time from the carrier reservoir to the active region, the population inversion factor, the injection current, the equivalent pseudorandom binary sequence length, the alpha-factor, the optical confinement factor, the operating data rate, the input pulse energy, and the continuous wave power in the presence of amplified spontaneous emission noise. The obtained results demonstrate that owing to the CR-SOA faster gain and phase recovery, the CR-SOA-DI is more suitable for realizing the OR logic gate at 100 Gb/s as it manages to achieve a more than acceptable Q-factor value of 9, compared to the unacceptable value of 3 when using the conventional SOA-DI.

1. Introduction

The OR is among the indispensable Boolean functions which are exploited in signal processing applications in the optical domain [1]. Owing to their compact size, small power consumption, wide gain bandwidth, and strong nonlinearity, semiconductor optical amplifiers (SOAs) constitute the primary choice for realizing the all-optical OR logic gate. This has been done with the assistance of interferometric configurations, either passive [2], or active [3]. Despite the SOA attractive characteristics, the slow SOA gain carrier recovery time limits its operation at higher speeds [4]. For this reason, researchers intensified their efforts in previous years to find a suitable alternative that works at higher rates with acceptable performance. These efforts have led to alternatives like the Quantum-Dot-SOA (QD-SOA) [5], the Photonic Crystal SOA (PC-SOA) [6], and the Reflective SOA (RSOA) [7]. Because the operating mechanism of these devices is different, there is no guarantee in advance that the target all-optical gate will be implemented with acceptable performance. This means that each SOA-based device should not be viewed as a general black box, but as a specific nonlinear switching entity that needs special treatment. Similarly, even if the switching configuration that incorporates some type of SOA-based device may have been well established, yet this does not mean either that an all-optical gate will be implemented both with logical correctness and high quality, unless a thorough investigation is conducted to confirm this fact. This approach can eventually open the road to alternative options of implementing all-optical gates, while offering designers multiple technological solutions to choose from. In the footsteps of these commendable efforts, we propose in this paper to employ the Carrier Reservoir SOA (CR-SOA) as an alternative technological approach for executing Boolean logic exclusively by means of light that owing to its inherently faster gain and phase response overcomes the normal SOA's response limitation and allows to execute all-optically the Boolean OR logic at a data rate of 100 Gb/s. CR-SOAs had so far been confined to classic signal amplification [8], and only recently have these devices been employed to implement all-optical logic gates [9,10], which for the first time include the OR. In this work, the CR-SOA is followed by a

* Corresponding authors.
E-mail addresses: amer@ciomp.ac.cn (A. Kotb), weili1@ciomp.ac.cn (W. Li).

https://doi.org/10.1016/j.optlastec.2021.107230
Received 30 November 2020; Received in revised form 20 April 2021; Accepted 10 May 2021
Available online 1 June 2021

delayed interferometer (DI) as in Ref. [2]. The DI creates a phase window whose duration is set by the shorter delay of the DI and which is beneficial for the quality of the output signal [1,4]. The CR-SOA-DI is compared to the conventional SOA-DI at 100 Gb/s through examining the quality factor (Q-factor) versus critical operating parameters, which include the transition time from the carrier reservoir to the active region, the population inversion factor, the injection current, the equivalent pseudorandom binary sequence (PRBS) length, the alpha-factor, the confinement factor, the operating data rate, the pulse energy, and the continuous wave (CW) power under the effect of amplified spontaneous emission (ASE) to obtain realistic results.

Compared to other schemes which have been deployed to realize the OR gate [11–14], such as the electro-optic-MZI (named henceforth Scheme 2-S2) [11,12] and plasmonic-MZI (named henceforth Scheme 3-S3) [13,14], the proposed scheme (named henceforth Scheme 1-S1) is better from several aspects. Compared to S2, the data between which the target Boolean function is executed are already in optical form, whilst in S2 they are not. This helps avoid power and time-consuming conversions between electrical and optical domain, and allows energy efficient, low latency and 'on-the-fly' signal processing, which are highly desirable features in real communication systems and networks. Moreover, implementations based on S2 suffer from inevitable trade-offs between switching energy, device size and footprint, and operating bandwidth [15], which poses stricter challenges towards scaling to higher line data rates than for S1. Furthermore, unlike S1, S2 requires proper adjustment between the switching voltage, the length of the interferometer arms and the separation between the electrodes to produce the level of differential phase shift required for switching [16]. This in turn may demand to follow an intricate setting procedure that becomes complicated when having to interconnect multiple gates to form large switching arrays or feedback configurations. In addition, supporting data rates as high as those with S1 requires using MZI lengths being roughly 2500 times smaller than the CR-SOA's active region length. Except for compromising fabrication reproducibility, this difference is also accompanied by the need to provide extra voltage supply and hence by an increased energy per switched bit. Compared to S3, S1 does not suffer from inherent insertion losses, unless resorting to special waveguide structures [17]. This fact makes more feasible using S1 the process of driving subsequent identical gates and building complex circuits and subsystems of enhanced functionality. It is also more mature and compatible with standard modern semiconductor fabrication methods. Compared to both S2 and S3, S1 allows more easily to perform optical signal processing functions on multiple channels using a single device. Additionally, S1 is amenable to the exploitation and simultaneous manipulation of multiple dimensions of the optical wave, i.e. amplitude, phase, wavelength, polarization, and space, thus offering more degrees of design freedom [18]. Overall, S1 competes favorably against S2 and S3 when implementing Boolean logic functions like the OR in terms of flexibility, tunability, configurability, scalability, and transparency, which are highly desirable characteristics that an ultrafast switching scheme must exhibit.

The outcome of this work can open new possibilities in the realization of all-optical gates, as well as in the design and implementation of sequential and combinational all-optical circuits and subsystems, which rely on them as core building blocks, at ultra-high speeds. It can also constitute a focus point for further research on the treated subject, given that in recent works reported on OR gate implementation either with well-established or rapidly developing, technologies, such as electro-optic modules and plasmonic waveguides [11–14], respectively, there are open issues concerning the presented results. Thus most of these works have shown static responses derived using computational electromagnetics methods to explain their proposed OR gate operation, which is supported by analogous performance metrics, such as the extinction ratio. However, they have not provided information about the pulse outcome of the considered Boolean logic function so as to be able to confirm that it is executed with logical correctness and with a high-quality profile. Furthermore, they have not provided evidence about whether their schemes can support operation for return-to-zero (RZ) data format, which is widely used in modern lightwave communications and inherently imposes a greater strain on the performance of such schemes. In this paper, we fill this gap in knowledge by reporting a complete set of results for the OR gate between RZ data under dynamic operating conditions, which have been obtained after assessing its ultrafast performance using the ultimate evaluation criterion of the Q-factor.

The conducted theoretical treatment can help understand the underlying operating mechanisms, predict functional behaviors, optimize working performances and form a basis for future studies on CR-SOA-based all-optical gates. It can also spur researchers to conduct experiments to verify our outcomes and exploit further the demonstrated potential of the CR-SOA-based all-optical OR gate.

2. Principle of operation

2.1. CR-SOA

Fig. 1 shows the CR-SOA band diagram. Similar to QD-SOAs, CR-SOAs allow to accelerate the speed of operation in which they are involved by exploiting the so-called 'carrier reservoir', but in a different physical way. Specifically, in the QD-SOA the faster response compared to a conventional SOA is due to the presence of the wetting layer, which acts as the carrier storage region, while the quantum dots (QDs) act as the active region [19]. Carriers depleted by the injected optical pulse in the QD ground state are replaced by fast carrier transfer from the wetting layer. As the injected current density is increased, more carriers are supplied in the wetting layer, which hence accelerates the speed of response. Therefore, the speed is determined by the relaxation time from the wetting layer to the quantum dot state. In CR-SOA, on the other hand, the carrier reservoir (CR) region is grown in the vicinity of the active region (AR), or alternatively the latter can include both the reservoir layer and the active layer [20]. When the CR is significantly populated, it supplies the active region with carriers with a transition time as fast as that of QD-SOA. This ultrafast transition dominates the gain dynamics, thus making the CR-SOA also exhibit an equally fast temporal gain and phase response as the QD-SOA. However, in CR-SOA there may exist more trade-offs, in terms of material composition and active region dimensions, between high performance and fast speed, which may compromise its speed enhancement capability compared to QD-SOAs. In fact, due to the limited available states in the QDs, the value of the inversion factor is much smaller in QD-SOAs, which makes them amenable to even faster operation. Still uniform QD-SOAs are also less technologically mature and more difficult to fabricate [8]. This essentially means that forming the required carrier reservoir with the available semiconductor processing techniques may be more feasible for CR-SOAs, which hence may be comparatively preferable with regard to

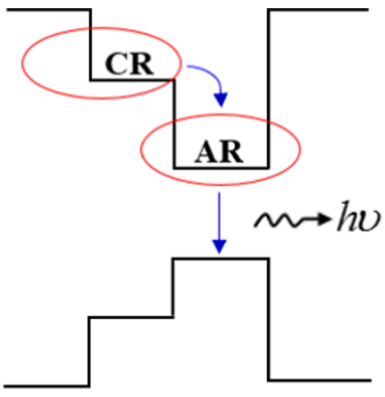

Fig. 1. CR-SOA band diagram.

reduced cost and complexity and better overall practicality.

The bandgap of the CR layer is larger than that of the AR region. When applying a driving current, carriers start to fill the available states in both AR and CR. When the injection current is low, the carrier density in the AR is larger than in CR. With the increase of the injection current, the CR accumulates sufficient carriers to function as a reservoir of supplied carriers. The incident photons are launched into the AR and collide with electrons to generate photons by stimulated emission. The carriers depleted in the AR by an energetic signal are rapidly replaced in the active region by the significantly populated CR. The transitions from the CR to the AR during this process can occur as fast as a few picoseconds, i. e. 05 – 5 ps [21], and hence accelerate the CR-SOA gain and phase response to the point that it renders feasible ultrafast switching of data without the performance restrictions imposed by ordinary SOAs. At higher launched signal intensities, the nonlinear intraband effects of carrier heating (CH) and spectral hole burning (SHB) also manifest on a short time scale of 0.7–1 ps.

2.2. OR gate

The schematic diagram of the all-optical OR logic gate using a CR-SOA followed by a DI is shown in Fig. 2.

To execute the OR operation using a CR-SOA-based DI, two data streams, A, B, and a continuous wave (CW) probe signal are combined and inserted in the active device. Signals A and B induce via CR-SOA cross-phase modulation phase shifts on the CW beam, which carries the information of the Boolean OR function. The CW signal coming out of the CR-SOA is further divided by a 3 dB optical coupler (OC) into two halves of equal intensity, which enter a DI. The DI creates a phase difference between the CW constituents by adjusting its delay time ($\Delta\tau$) and phase bias ($\Delta\Phi$). The role of the delay line, $\Delta\tau$, is to control the phase window which is opened by the difference between the phases of the direct and offset replicas of the signal switched from the CR-SOA and traveling along the DI upper and lower arms, respectively. More specifically, the CW components, which represent the '0's, and on which a stronger or weaker phase shift has been imparted, either by A = '1', B = '1', in the former, and A = '1', B = '0' and vice versa, in the second case, are arranged to fall within this formed window so that they are transmitted at the DI output, thus producing logic '1's. Because the CR-SOA gain and phase perturbations that these CW components have experienced are not uniform, as they have been caused by different binary combinations, by further adjusting through the DI phase shifter the magnitude of interference at the DI output it is possible to compensate for these intensity fluctuations and eventually obtain '1's of uniform peak amplitude, as desired. In contrast, the CW components which represent the '1's, and on which no phase shift has been induced, are forced to lie outside the phase window, thus being suppressed at the DI output and resulting in '0's. Accordingly, the truth table of the OR gate is realized, which is the pursued goal.

3. Modeling

The dynamic operation of the CR-SOA is modeled through the following time-dependent first-order coupled differential equations, which account for the carrier recombination between CR and AR as well as CH and SHB ultrafast nonlinear processes [8–10]:

$$\frac{dh_{AR}(t)}{dt} = \frac{h_{CR}(t)-h_{AR}(t)}{\tau_t(1+\eta)} + \frac{\eta h_0}{\tau_c(1+\eta)} - \frac{h_{AR}(t)}{\tau_c} - (exp[h_{AR}(t) + h_{CH}(t) + h_{SHB}(t)] - 1)\frac{P_{in,\ CR-SOA}(t)}{E_{sat}} \quad (1)$$

$$\frac{dh_{CR}(t)}{dt} = -\frac{\eta(h_{CR}(t)-h_{AR}(t)}{\tau_t(1+\eta)} + \frac{h_0-h_{CR}(t)}{\tau_c(1+\eta)} - \frac{h_{CR}(t)}{\tau_c} \quad (2)$$

$$\frac{dh_{CH}(t)}{dt} = -\frac{h_{CH}(t)}{\tau_{CH}} - \frac{\varepsilon_{CH}}{\tau_{CH}}(exp[h_{AR}(t)+h_{CH}(t)+h_{SHB}(t)]-1)P_{in,CR-SOA}(t) \quad (3)$$

$$\frac{dh_{SHB}(t)}{dt} = -\frac{h_{SHB}(t)}{\tau_{SHB}} - \frac{\varepsilon_{SHB}}{\tau_{SHB}}(exp[h_{AR}(t) + h_{CH}(t) + h_{SHB}(t)] - 1)P_{in,\ CR-SOA}(t) - \frac{dh_{AR}(t)}{dt} - \frac{dh_{CH}(t)}{dt} \quad (4)$$

where functions 'h' are the CR-SOA's gain integrated over its length for the carrier recombination between AR (h_{AR}) and CR (h_{CR}), CH (h_{CH}), and SHB (h_{SHB}). τ_t is the transition time from the CR layer to the AR layer and τ_c is the carrier lifetime in both AR and CR. The quantity η is the population inversion factor defined as the ratio of the carrier densities in AR and CR, i.e. $\eta = N_{AR}/N_{CR}$. $h_0 = \ln[G_0]$, where G_0 is the unsaturated power gain related to other parameters via $G_0 = \alpha\Gamma(I\tau_c/eV - N_{tr})L$ [4], where α is the differential gain, Γ is the optical confinement factor, I is the injection current, e is the electron charge, V is the volume of the AR, N_{tr} is the transparency carrier density, and L is the length of the AR. E_{sat} is the saturation energy given by $E_{sat} = P_{sat}\tau_c = wdh\omega_0/\alpha\Gamma$ [4], where P_{sat} is the saturation energy, w & d are the width and thickens of the AR, respectively, $\hbar$ is the normalized Planck's constant (i.e. $\hbar = h/2\pi$), and ω_0 is the central optical frequency. τ_{CH} and τ_{SHB} are the temperature relaxation rates for the CH and SHB, respectively. ε_{CH} and ε_{SHB} are the nonlinear gain suppression factors for the CH and SHB, respectively. The CR-SOA total gain is then given by:

$$G_{CR-SOA}(t) = exp[h_{AR}(t) + h_{CH}(t) + h_{SHB}(t)] \quad (5)$$

The phase change induced on an input CW signal inside the CR-SOA is given by:

$$\Phi_{CR-SOA}(t) = -0.5(\alpha h_{AR}(t) + \alpha_{CH} h_{CH}(t)) \quad (6)$$

where α is the traditional linewidth enhancement factor, namely α-factor, and α_{CH} is the linewidth enhancement factor for CH. The contribution to the total phase of SHB is null, as implied in Eq. (6), i.e. $\alpha_{SHB} = 0$ [4–7].

The optical power ($P_{in,\ CR\text{-}SOA}(t)$) of the input data A, B, is assumed to exhibit a Gaussian-shaped profile comprising of RZ pulses having a FWHM (full-wave half maximum) pulse width (τ_{FWHM}), energy (E_0), length of carried pseudorandom binary sequence (PRBS) $N = 2^7\text{-}1$, namely equivalent PRBS length of 7, and bit period (T), which is the inverse of the operating data rate:

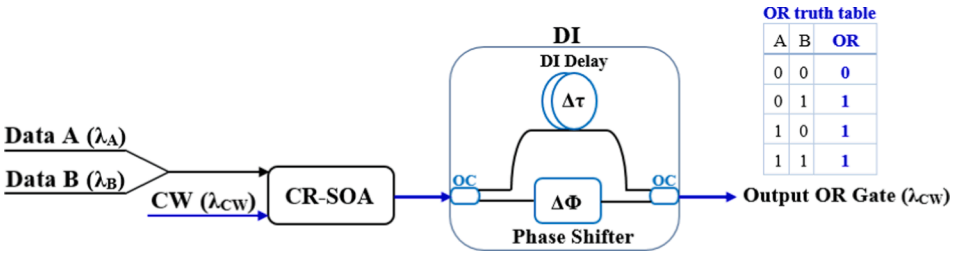

Fig. 2. Schematic diagram and truth table of OR logic gate using CR-SOA-assisted DI. OC: 3 dB optical coupler.

$$P_{A,B}(t) = \sum_{n=1}^{N} a_{n(A,B)} \frac{2\sqrt{ln[2]}\,E_0}{\sqrt{\pi}\,\tau_{FWHM}} \exp\left[-\frac{4ln[2](t - nT)^2}{\tau_{FWHM}^2}\right] \quad (7)$$

where $\alpha_{n(A,B)}$ denotes the n-th pulse inside the PRBS, which can take a binary value of '1' or '0'. Since in the employed scheme the input signals A, B, and the continuous wave (CW) beam of power P_{CW} are coupled into a single CR-SOA, the total input power in the CR-SOA is :

$$P_{in,\ CR-SOA}(t) = P_A(t) + P_B(t) + P_{CW} \quad (8)$$

The power coming out of the DI is given by the following basic interferometric formula [4,6]:

$$P_{OR}(t) = 0.25\left(P_{out,\ CR-SOA}(t) + P_{out,\ CR-SOA}(t-\Delta\tau) - 2\sqrt{P_{out,\ CR-SOA}(t)\,P_{out,\ CR-SOA}(t-\Delta\tau)}\ cos\left[\Phi_{out,\ CR-SOA}(t) - \Phi_{out,\ CR-SOA}(t-\Delta\tau) + \Delta\Phi\right]\right) \quad (9)$$

where $P_{out,\ CR-SOA}(t)$ is the CR-SOA output power defined as $P_{out,\ CR-SOA}(t) = G_{CR-SOA}(t)\,P_{CW}$.

4. Results

The performance of the considered Boolean operation is evaluated at 100 Gb/s by deriving and interpreting curves of the Q-factor variation against critical operating parameters, under the effect of ASE noise in order to achieve results close to reality. It should be noted that the data rate of 100 Gb/s is investigated not for any fundamental reason but because it is in line with current trends in modern optical systems and networks, while it allows to sufficiently test, assess and validate the ultrafast switching potential of CR-SOAs. For acceptable performance, a Q-factor value of 6 is required to ensure that the related bit-error-rate [22] is kept below 10^{-9} [5–7]. For this purpose, Eqs. (1)-(9) are combined and run by using Adams' numerical method implemented in Wolfram Mathematica software. This is a multistep method for solving first-order differential equations, as in our case, which approximates the integrand with a polynomial and then uses the latter to evaluate the integral [23]. The default parameter values in the simulation are cited in Table 1 [1–10] and are used for both CR-SOA and SOA for a fair comparison. Besides, these values agree with those reported in the literature for (CR-) SOA with the same geometrical and optical characteristics as in this work.

Table 1
Simulation default parameters [1–10].

Symbol	Definition	Value	Unit
E_0	Pulse energy	0.7	pJ
τ_{FWHM}	Pulse width	1	ps
T	Bit period	10	ps
N	PRBS length	127	-
λ_A	Wavelength of data A	1559	nm
λ_B	Wavelength of data B	1546	nm
λ_{CW}	Wavelength of CW	1554	nm
P_{CW}	Power of CW	0.3	mW
I	Injection current	200	mA
P_{sat}	Saturation power	10	mW
τ_c	Carrier lifetime	200	ps
τ_t	Transition lifetime from CR to AR	5	ps
η	population inversion factor	0.3	-
α	α-factor	5	-
α_{CH}	CH linewidth enhancement factor	1	-
α_{SHB}	SHB linewidth enhancement factor	0	-
ε_{CH}	CH nonlinear gain suppression factor	0.2	W^{-1}
ε_{SHB}	SHB nonlinear gain suppression factor	0.2	W^{-1}
τ_{CH}	Temperature relaxation rate	0.3	ps
τ_{SHB}	Carrier-carrier scattering rate	0.1	ps
Γ	Optical confinement factor	0.3	-
ɑ	Differential gain	2×10^{-16}	cm^2
N_{tr}	Transparency carrier density	10^{18}	cm^{-3}
L	Length of AR	500	μm
d	Thickness of AR	0.3	μm
w	Width of AR	3	μm
G_0	Unsaturated power gain	30	dB
N_{SP}	Spontaneous emission factor	2	-
υ	Optical frequency	193.55	THz
B_0	Optical bandwidth	2	nm
ħ	Normalized Planck's constant	1.05×10^{-34}	J.s
Δτ	DI delay time	0.2	ps
ΔΦ	DI phase bias	π	rad

Fig. 3 shows the gain and phase recovery of both CR-SOA and conventional SOA for 100 Gb/s input optical signal. From this figure, a faster gain recovery and phase resulting from the ultrafast transition due to the CR layer is observed for the CR-SOA. Moreover, the gain and phase variation quickly reaches a steady-state, in contrast to the regular SOA for which the corresponding temporal evolution suffers from intense fluctuations. Thus the CR-SOA is qualified as a more suitable nonlinear device for supporting higher speed Boolean operations compared to an ordinary SOA, whose response is limited by the slow dynamics.

Figs. 4 and 5 show the profiles of the input data streams A and B, the output of the OR logic gate, and the OR eye diagram at 100 Gb/s using CR-SOA- and conventional SOA-assisted DI, respectively. These results reveal that using the CR-SOA-DI allows to realize the all-optical OR logic gate with a higher Q-factor than using the conventional SOA-DI. In fact, the Q-factor is 9 when using the CR-SOA-DI as opposed to 3 when using the SOA-DI. The tripled Q-factor achieved with the CR-SOA-DI is attributed to the ultrafast transition time from the occupied CR level to the AR level.

Both the transition time from CR to AR (τ_t) and the population inversion factor (η) play a significant role in the operation of the CR-SOA. Therefore, it is necessary to investigate their influence on the performance of the OR gate, which is done within the frame of Fig. 6. A shorter τ_t leads to faster recovery and thus higher Q-factor, as shown in Fig. 6(a). τ_t has been measured to be in the range of ~ 0.5 to 5 ps in GaAs [21]. On the other hand, the quantity η defined as the ratio of carrier

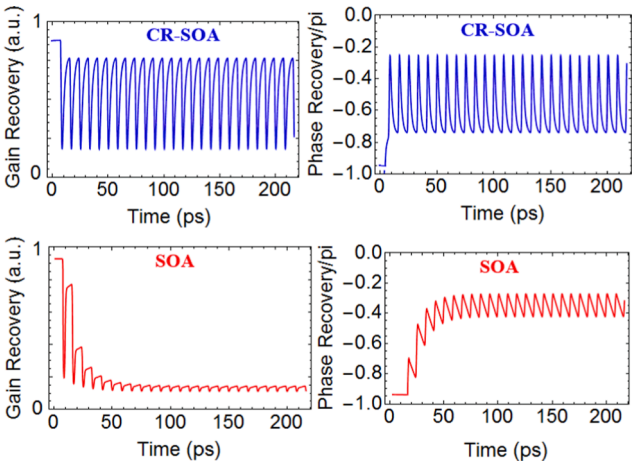

Fig. 3. Gain and phase recovery for CR-SOA and normal SOA at 100 Gb/s.

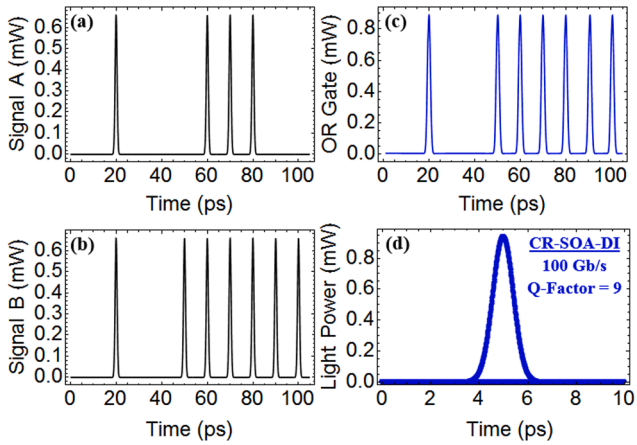

Fig. 4. Numerical results using CR-SOA-DI at 100 Gb/s. (a) Input data stream A, (b) input data stream B, (c) output of OR gate, and (d) corresponding eye diagram with Q-factor = 9.

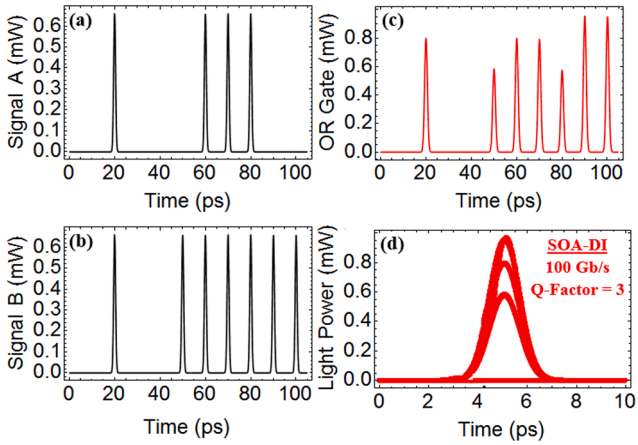

Fig. 5. Numerical results using conventional SOA-DI at 100 Gb/s. (a) Input data stream A, (b) input data stream B, (c) output of OR gate, and (d) corresponding eye diagram with Q-factor = 3.

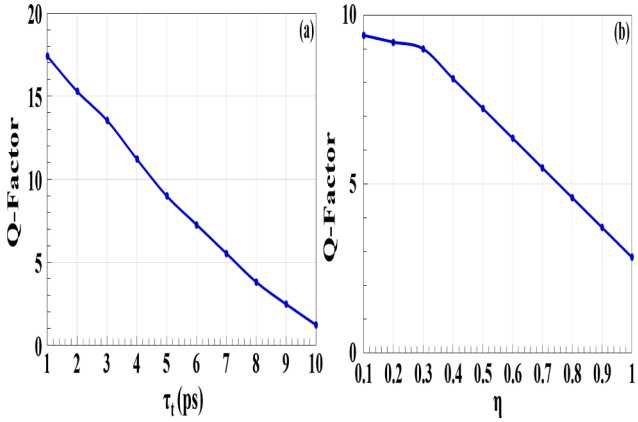

Fig. 6. Calculated Q-factor of OR gate at 100 Gb/s versus CR-SOA (a) transition time from CR to AR (τ_t) and (b) population inversion factor (η).

densities in AR and CR ($\eta = N_{AR}/N_{CR}$) is a measure of the amount of carriers available for fast gain recovery. Therefore, for a small η, the CR population is high and hence the gain recovery is faster, resulting in a higher Q-factor, as shown in Fig. 6(b).

The bias current plays a decisive role in the process of amplification

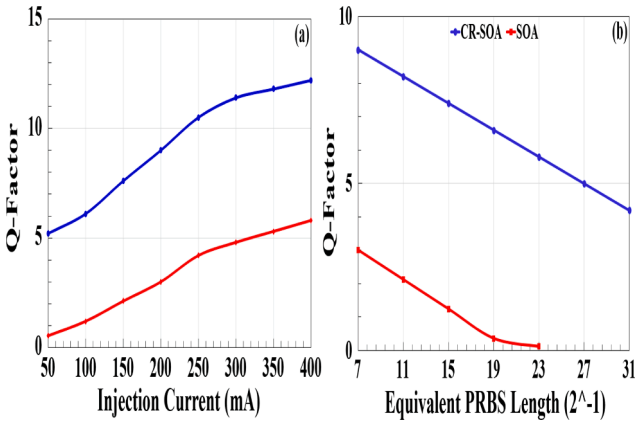

Fig. 7. Calculated Q-factor of OR logic gate at 100 Gb/s versus (a) injection current and (b) equivalent PRBS length using CR-SOA- and SOA-based DI.

and switching. Fig. 7(a) shows the dependence of the Q-factor on the injection current for the OR logic gate using CR-SOA- and SOA-based DI at 100 Gb/s. When current is applied to the CR-SOA, the carriers start filling the available states in both AR and CR. At low injection current, the AR carrier density is higher than that in CR because the quasi-Fermi level is close to the AR band edge. While at high injection current, the carrier density in CR becomes higher than in AR due to the motion of quasi-Fermi level up over the CR edge band [8]. Since more carriers are injected into the CR at high current, thereby allowing for faster recovery and refilling for the AR layer after depleting by a strong input pulse, this leads accordingly to an increase in the Q-factor, as shown in Fig. 7(a). In comparison, the performance of the OR gate based on the conventional SOA lacks significantly behind even for high current values which are favored for accelerated operation. Fig. 7(b) shows the variation of the Q-factor against the equivalent PRBS length for the OR operation using CR-SOA- and SOA-based DI at 100 Gb/s. The term 'equivalent' in the horizontal axis of the diagram refers to the number of consecutive '0's and '1's that corresponds to each order of PRBS. The Q-factor is decreased with an increase in the equivalent PRBS length for both considered amplifiers. This happens because in this case the operation of the logic gate is stressed more, since the risk of generating errors becomes potentially higher due to the protracted '0's and '1's [24]. Thus, Fig. 7(b) confirms that the CR-SOA enables operation of the OR gate for longer PRBS data than the SOA, while the latter is very sensitive to the extent of this digital content and does not allow to obtain acceptable performance.

The Q-factor is considerably increased for both amplifiers with

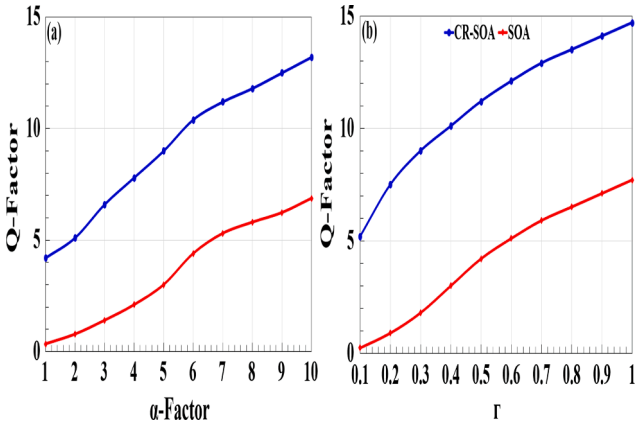

Fig. 8. Calculated Q-factor of OR logic gate at 100 Gb/s versus (a) traditional linewidth enhancement factor (α-factor) and (b) optical confinement factor (Γ) using CR-SOA- and SOA-based DI.

higher traditional linewidth enhancement factor (α-factor) and optical confinement factor (Γ), as shown in Fig. 8. According to Eq. (6), α-factor affects the magnitude of the phase response. The latter is stronger in the CR-SOA than in the SOA, therefore the Q-factor is more acceptable, even for small values of this parameter, in the CR-SOA than in the conventional SOA, as shown in Fig. 8(a). Similar behavior is seen in Fig. 8(b) for the Q-factor versus the confinement factor Γ for both structures. Since by definition Γ is the ratio of the power flow inside the active region to the total power flow [25], this means that for small Γ less power is confined into the active region, which affects accordingly the saturation level of the device and decreases the Q-factor. Notably, the CR-SOA maintains the Q-factor acceptable even for small values of Γ as a result of the optimum utilization of the power flow.

Both SOA types exhibit ASE noise, which affects the performance of the OR logic gate and so its effect cannot be neglected. For this reason, the impact of ASE on the performance of the considered function using CR-SOA- and SOA-based-DI at 100 Gb/s has been examined and is shown in Fig. 9(a). The ASE power is calculated in the optical bandwidth (B_0) using $P_{ASE} = N_{SP}\,(G_0 - 1)\,2\pi h\upsilon B_0$ [4,7] and is numerically added to the OR output power given by Eq. (9). The Q-factor is decreased with the increase in the ASE power for both CR-SOA and conventional SOA, but it is noticed that the CR-SOA enables to achieve acceptable performance even at higher ASE contribution, while this is not possible with the conventional SOA for which the same effect is rather detrimental. This happens because the CR-SOA faster gain dynamics suppress ASE to the extent that it does not affect the performance irreversibly. With regard now to the data rate that the CR-SOA can operate while keeping the OR gate's performance acceptable, Fig. 9(b) shows that this is possible up to a working point of 140 Gb/s, at which an acceptable Q-factor of 6.2 is achieved, while the limit for the conventional SOA is 1.75 times lower. Operation at higher data rates, such as 160 Gb/s or even 250 Gb/s, is possible provided that the CR-SOA is biased with higher current, energy of the data pulses is smaller, and the DI delay is shorter. The first two actions are required in order to be able to compensate for the reduction of the phase shift induced on the CW beam by the ultra-high-speed data signals and maintain the necessary level for proper switching [26], while the latter because for proper operation the duration of the DI phase window should scale inversely with the data rate so as to be able to handle temporally narrower signals [27]. With these conditions, which can be satisfied in practice with the relevant technology available for driving CR-SOAs, generating and boosting data pulses and designing DIs, respectively, the Q-factor can become acceptable at 250 Gb/s for I = 450 mA, E_0 = 0.2 pJ, and Δτ = 0.1 ps, respectively. Overall, these results prove the ability of the CR-SOA to operate at a higher ASE level and higher data rate compared to the conventional SOA.

To get further insight into the performance of the OR logic gate, the

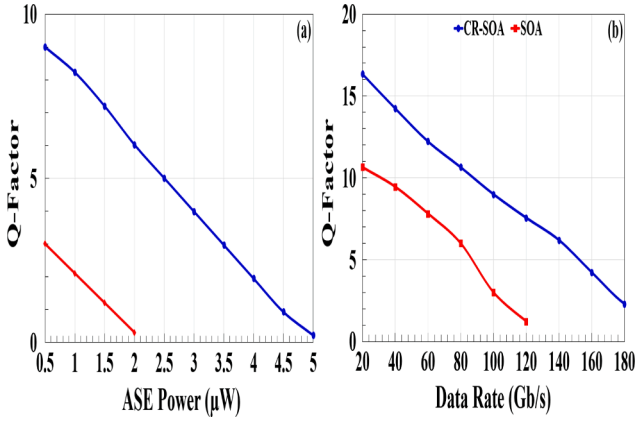

Fig. 9. Calculated Q-factor of OR logic gate versus (a) amplified spontaneous emission (ASE) power at 100 Gb/s and (b) operating data rate using CR-SOA- and SOA-based DI.

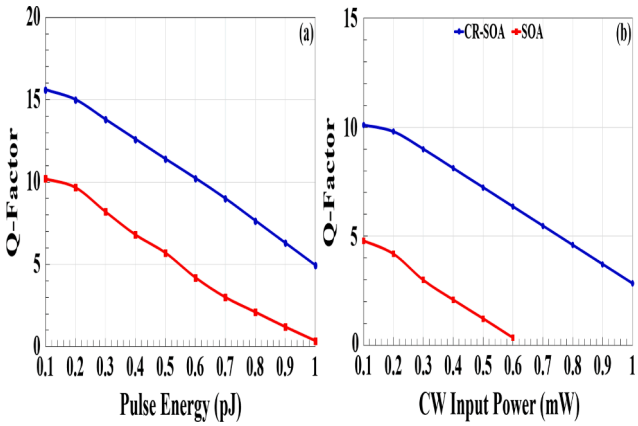

Fig. 10. Calculated Q-factor of OR logic gate versus (a) input pulse energy and (b) CW input power using CR-SOA- and SOA-based DI.

Q-factor against the input pulse energy and CW input power using both CR-SOA- and SOA-DI at 100 Gb/s is depicted in Fig. 10. As seen from Fig. 10(a), the CR-SOA-DI scheme achieves a higher Q-factor and hence better performance than the SOA-DI for the same pulse energy. The increase of the input pulse energy causes the depletion of carriers and thus reduces the Q-factor, but thanks to the CR layer in the CR-SOA the Q-factor is higher and remains acceptable for almost the whole span of input pulse energies, which is not possible with the conventional SOA-based DI. Similar behavior is seen in Fig. 10(b) for the Q-factor versus the CW input power. Although this parameter has physically a direct impact on both CR-SOA and regular SOA dynamical behavior, yet the former device is more tolerant than the latter to changes incurred across a wider range, which is reflected on the far better and acceptable Q-factor.

Finally, we compare the performance of the OR logic operation in terms of the Q-factor achieved using the CR-SOA against the same metric obtained with other SOA-based schemes. Table 2 highlights the superiority of the CR-SOA over other SOA-based schemes at the same data rate. Also, this Table suggests that the data rate could be increased using the CR-SOA when placing QDs in its active region or integrating it with PCs or when the effect of the two-photon absorption (TPA) is concurrently exploited.

The limitations of our theoretical analysis compared to other published approaches mainly concern:

a)The one-dimensional dependence, and accordingly, the method of solution, of the model used to simulate and investigate the performance of the CR-SOA and subsequently of the OR gate in which it is employed as a nonlinear element. According to this approach, the CR-SOA is treated as a spatially concentrated device by dropping the dependence on the longitudinal dimension, 'z', through the integration of the CR-SOA gain over its length, 'L', represented by the different 'h' functions in differential equations (1)-(4), which hence are ordinary of only one

Table 2
Comparison of OR operation for different SOA-based schemes and data rates.

Scheme	Data rate (Gb/s)	Q-factor	Ref.
SOA-DI	80	5.48	[2]
	100	3	This work
	160	5.2	[6]
SOAs-MZI	80	11	[3]
CR-SOA-DI	100	9	This work
SOA-DI-TPA	250	9	[28]
QD-SOA-DI	160	9	[5]
	250	6.5	[5]
	1000	45.5	[29]
	2000	8.2	[30]
QD-SOA-DI-TPA	2000	15	[30]
PC-SOA-DI	160	23	[6]

independent variable, time ('t'). This approach reduces the computational complexity and allows to calculate the time-dependent gain and phase shift experienced by the CW signal inside the CR-SOA through the analytical expressions of relationships (5) and (6), respectively. This approach, however, which was originally established and validated in [31] for conventional SOAs and later on properly adapted to the case of CR-SOAs [8], does not allow to investigate and reveal the influence of factors, such as the CR-SOA length, which may affect the CR-SOA optical modulation bandwidth and accordingly its capability to support ultrafast operation in the configurations where it is employed as nonlinear element [32].

b)The treatment of the CR-SOA small-signal gain and saturation energy as wavelength-independent parameters. This assumption applies for picosecond optical pulses whose spectral width is much smaller than the frequency detuning between data A, B, and the CW beam, which hence holds in our case since the former value is approximately 0.44 GHz for the considered unchirped Gaussian-shaped 1 ps-wide pulses while the latter is as low as 625 GHz for the involved signals wavelengths cited in Table 1. For this reason, it is justified not to use some polynomial approximation of the gain spectrum [33], which would only increase the model's complexity without making any significant difference in the obtained results. Still, this approach does not allow us to investigate the impact of the input signals wavelength so that we could determine a range of it that would correspond to optimum gate performance.

c)The treatment of the CR-SOA lifetime parameters as constants of the carrier density. This approach also simplifies the computational process and is valid in the saturation regime at which the CR-SOA is held by the constantly applied CW signal after being brought there due to the combined action of the two strong data signals. However, an expanded theoretical investigation and specification of the conditions under which the CR-SOA can also operate in different saturation levels, or have its ultrafast optical response being intensively modulated by an external excitation, so as to uncover its full switching potential for all-optical signal processing purposes, would require approximating the carriers recombination rate by a suitable polynomial, instead of a linear one [32].

5. Conclusion

In this research, we theoretically studied and confirmed the possibility of executing the all-optical Boolean OR logic at 100 Gb/s using a CR-SOA-assisted DI. A thorough and fair comparison was made between the CR-SOA- and SOA-assisted DI by examining the variation of the Q-factor against various key operating parameters, including the effect of the ASE noise. The numerical outcomes revealed the better performance of the OR gate when implemented with the CR-SOA since a Q-factor of 9 was achieved compared to 3 with the conventional SOA. These results can spur the employment of CR-SOAs as nonlinear elements for the design and implementation of ultrafast photonic circuits and subsystems.

Declaration of Competing Interest

The authors declare that they have no known competing financial interests or personal relationships that could have appeared to influence the work reported in this paper.

Acknowledgments

Amer Kotb sincerely acknowledges the CAS President's International Fellowship Initiative (Grant No. 2019FYT0002) and the Talented Young Scientist Program in China for supporting this work.

References

[1] K.E. Zoiros, All-optical logic gates with quantum-dot semiconductor optical amplifiers, Proc. International Conference on Transparent Optical Networks (ICTON), art. no. 6602760, 2013.
[2] Q. Wang, H. Dong, G. Zhu, H. Sun, J. Jaques, A.B. Piccirilli, N.K. Dutta, All-optical logic OR gate using SOA and delayed interferometer, Opt. Commun. 260 (2006) 81–86.
[3] A. Kotb, K.E. Zoiros, G. Guo, Numerical investigation of all-optical logic OR gate at 80 Gb/s with dual pump-probe semiconductor optical amplifier (SOA)-assisted Mach-Zehnder interferometer (MZI), J. Comp. Electron. 18 (2019) 271–278.
[4] N.K. Dutta, Q. Wang, Semiconductor Optical Amplifiers, second ed., World Scientific, Singapore, 2013.
[5] H. Sun, Q. Wang, H. Dong, N.K. Dutta, All-optical logic performance of quantum-dot semiconductor amplifier-based devices, Microwave Opt. Technol. Lett. 48 (2006) 29–35.
[6] A. Kotb, K.E. Zoiros, C. Guo, Ultrafast performance of all-optical AND and OR logic operations at 160 Gb/s using photonic crystal semiconductor optical amplifier, Opt. Laser Technol. 119 (2019), 105611.
[7] A. Kotb, C. Guo, 120 Gb/s all-optical NAND logic gate using reflective semiconductor optical amplifiers, J. Mod. Opt. 67 (2020) 1138–1144.
[8] H. Sun, Q. Wang, H. Dong, G. Zhu, N.K. Dutta, J. Jaques, Gain dynamics and saturation property of a Semiconductor Optical Amplifier with a carrier reservoir, IEEE Photon. Technol. Lett. 18 (2006) 196–198.
[9] A. Kotb, K.E. Zoiros, W. Li, Numerical Study of carrier reservoir semiconductor optical amplifier-based all-optical XOR logic gate, J. Mod. Opt. 68 (2021) 161–168.
[10] A. Kotb, Ultrafast carrier reservoir semiconductor optical amplifiers-based all-optical AND logic gate, Opt. Eng. 60 (2021), 026104.
[11] H. Alizadeh, A. Rashidi, Implementation of optical OR and NOR gates using Mach-Zehnder interferometers, J. Phys. Commun. 4 (2020), 085014.
[12] S. Awasthi, A. Biswas, S.K. Metya, A. Majumder, Optical configuration of modified Fredkin gate using lithium-niobate-based Mach-Zehnder interferometer, Appl. Opt. 59 (2020) 7083–7091.
[13] A. Pal, M.Z. Ahmed, S. Swarnakar, An optimized design of all-optical XOR, OR, and NOT gates using plasmonic waveguide, Opt. Quant. Electron. 53 (2021) 84.
[14] L. Singh, G. Zhu, G.M. Kumar, D. Revathi, P. Pareek, Numerical simulation of all-optical logic functions at micrometer scale by using plasmonic Metal-Insulator-Metal (MIM) waveguides, Opt. Laser Technol. 135 (2021), 106697.
[15] H. Lin, O. Ogbuu, J. Liu, L. Zhang, J. Michel, J. Hu, Breaking the energy-bandwidth limit of electrooptic modulators: Theory and a device proposal, J. Lightwave Technol. 31 (2013) 4029–4036.
[16] S. Kumar, G. Singh, A. Bisht, S. Sharma, A. Amphawan, Proposed new approach to the design of universal logic gates using the electro-optic effect in Mach-Zehnder interferometers, Appl. Opt. 54 (2015) 8479–8484.
[17] H.M.G. Wassel, D. Dai, M. Tiwari, J.K. Valamehr, L. Theogarajan, J. Dionne, F. T. Chong, T. Sherwood, Opportunities and challenges of using plasmonic components in nanophotonic architectures, J. Emerg. Sel. Top. Circuits Syst. 2 (2012) 154–168.
[18] A.E. Willner, A. Fallahpour, F. Alishahi, Y. Cao, A. Mohajerin-Ariaei, A. Almaiman, P. Liao, K. Zou, A.N. Willner, M. Tur, All-optical signal processing techniques for flexible networks, J. Lightwave Technol. 37 (2019) 21–35.
[19] E. Dimitriadou, K.E. Zoiros, On the feasibility of 320 Gb/s all-optical AND gate using quantum-dot semiconductor optical amplifier-based Mach-Zehnder interferometer, Prog. Electromagn. Res. B (PIERS) 50 (2013) 113–140.
[20] M. Sorimachi, H. Iwasaki, T. Miyamoto, Theoretical investigation of high speed SOA using recombination-controlled carrier reservoir, in Proceedings Conference Laser and Electro-Optics Pacific Rim (CLEO-PR) 2013 ThK3-6.
[21] T. Furata, in Semiconductors & Semimetals Vol. 39, Ch. 3. Academic Press, New York, 1993.
[22] S. Thapa, X. Zhang, N.K. Dutta, Effects of two-photon absorption on pseudo-random bit sequence operating at high speed, J. Mod. Opt. 66 (2019) 100–108.
[23] H. Jeffreys, B.S. Jeffreys, The Adams'-Bashforth Method, 3rd ed., Cambridge University Press, England, 1988.
[24] T. Siarkos, K.E. Zoiros, D. Nastou, On the feasibility of full pattern-operated all-optical XOR gate with single semiconductor optical amplifier-based ultrafast nonlinear interferometer, Opt. Commun. 282 (2009) 2729–2740.
[25] Y. Huang, Z. Pan, R. Wu, Analysis of the optical confinement factor in semiconductor lasers, J. Appl. Phys. 79 (1996) 3827–3830.
[26] Y. Ueno, S. Nakamura, K. Tajima, Nonlinear phase shifts induced by semiconductor optical amplifiers with control pulses at repetition frequencies in the 40–160-GHz range for use in ultrahigh-speed all-optical signal processing, J. Opt. Soc. Am. B 19 (2002) 2573–2589.
[27] A. Kotb, K.E. Zoiros, C. Guo, 320 Gb/s all-optical XOR gate using semiconductor optical amplifier-Mach–Zehnder interferometer and delayed interferometer, Photon Netw. Commun. 38 (2019) 177–184.
[28] A. Kotb, Ultrafast all-optical logic OR gate based on two-photon absorption with a semiconductor optical amplifier-assisted delayed interferometer, Korean J. Phys. Soc. 68 (2016) 201–205.
[29] A. Kotb, Simulation of high-quality-factor all-optical logic gates based on quantum-dot semiconductor optical amplifier at 1 Tb/s, Optik 127 (2016) 320–325.
[30] A. Kotb, K.E. Zoiros, C. Guo, 2 Tb/s all-optical gates based on two-photon absorption in quantum dot semiconductor optical amplifiers, Opt. Laser Technol. 112 (2019) 442–451.

[31] D. Cassioli, S. Scotti, A. Mecozzi, A time-domain computer simulator of the nonlinear response of semiconductor optical amplifiers, IEEE J. Quantum Electron. 36 (2000) 1072–1080.
[32] R. Gutiérrez-Castrejón, L. Schares, L. Occhi, G. Guekos, Modeling and measurement of longitudinal gain dynamics in saturated semiconductor optical amplifiers of different length, IEEE J. Quantum Electron. 36 (2000) 1476–1484.
[33] K. Obermann, S. Kindt, D. Breuer, K. Petermann, Performance analysis of wavelength converters based on cross-gain modulation in semiconductor optical amplifiers, J. Lightwave Technol. 16 (1998) 78–85.